Atmospheric Forcing Conducive for the Adriatic 25 June 2014 Meteotsunami Event

Kristian Horvath, Jadranka Šepić & Maja Telišman Prtenjak

Pure and Applied Geophysics
pageoph

ISSN 0033-4553

Pure Appl. Geophys.
DOI 10.1007/s00024-018-1902-1

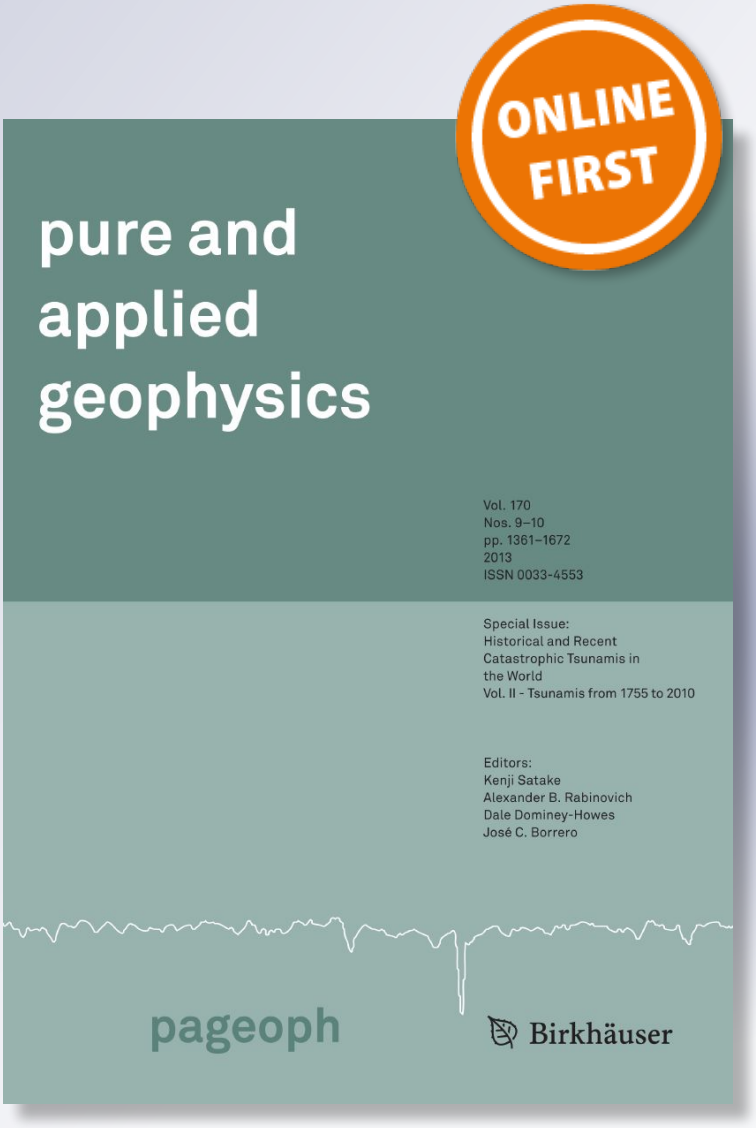

Springer

Pure Appl. Geophys.

https://doi.org/10.1007/s00024-018-1902-1

Pure and Applied Geophysics

Atmospheric Forcing Conducive for the Adriatic 25 June 2014 Meteotsunami Event

Kristian Horvath,[1] Jadranka Šepić,[2] and Maja Telišman Prtenjak[3]

Abstract—We analyze atmospheric conditions conducive for a meteotsunami event that occurred in the Adriatic on 25 June 2014. This was the most intensive of a series of meteotsunami events which occurred in the Mediterranean and Black Seas during 23–27 June 2014 period. Considerable sea-level oscillations were observed in several eastern Adriatic harbors with a maximum wave height of around 3 m and period of approximately 20 min observed in Vela Luka harbor, Korčula Island, Croatia. Observational analysis of the event utilizes available in situ and remote sensing measurements. For a more detailed insight into the structure of the atmosphere we reproduced the event with the WRF model configured at a sub-kilometer grid spacing. Observational and simulated data both demonstrate that sea-level oscillations in Vela Luka harbor were caused by rapid air–pressure perturbations with amplitudes of up to 4 hPa and a maximal rate of air pressure change above 2 hPa/5 min. Around the time pressure perturbations affected the area, pressure distribution was affected by both convection and internal gravity waves, with both wave-CISK and wave duct promoting maintenance of pressure perturbations. This makes the 2014 Adriatic event the first known meteotsunami event in the Mediterranean and Black Seas during which both of these maintenance mechanisms acted jointly. Finally, simulations performed in this event represented meteotsunami-related pressure perturbations at the adequate time and location, which is a step forward in the ability of atmospheric models to assist early warning meteotsunami systems for the Mediterranean and the Black Seas.

Key words: Meteotsunami, Adriatic Sea, wave-CISK, wave duct, WRF.

1. Introduction

A number of tsunami-like waves hit middle Adriatic harbors during 25 and 26 June 2014 (Šepić et al. 2015, 2016). First to be hit was Vela Luka harbor on the island of Korčula, where 3-m-high waves of ~ 20-min period appeared during early morning hours of 25 June (starting around 06:30 UTC). Later the same day, around 11:00 UTC, tsunami waves accompanied by strong ocean currents were observed in Rijeka Dubrovačka bay, 85 km to the east of Vela Luka. Several hours later, strong sea-level oscillations started at the island of Hvar, with tsunami waves of up to 1.5 m height striking Stari Grad (reaching maximum around 13:00 UTC) and Vrboska (reaching maximum around 15:00 UTC) harbors. During midday next day, tsunami waves of somewhat smaller height (up to 1.0 m) hit Viganj and Ston, both on Pelješac peninsula. All hit locations are shown in Fig. 1. Research decisively proved all these waves to be meteotsunamis (Šepić et al. 2015, 2016), tsunami-like waves of atmospheric origin which are commonly generated by intense and sudden changes of air pressure (Monserrat et al. 2006). Following the event, related ocean and atmospheric observational data were studied in detail, and observed and measured sea-level oscillations were reproduced using both synthetic and measured series of atmospheric pressure (Šepić et al. 2016). It was shown that numerous atmospheric pressure disturbances of limited horizontal dimensions [O(10 km × 10 km)] and short duration [O(1 h)] traversed the Adriatic Sea during 25 and 26 June, while at the same time generating multiple meteotsunami waves which further intensified to destructive heights at some particular locations. Exact nature of these air pressure disturbances remained unknown.

Meteotsunamis are known phenomena in the Adriatic Sea, with an exceptional event occurring every 5–10 years (Orlić 2015). The strongest of the known world meteotsunamis happened precisely in Vela Luka: during morning hours of 21 June 1978 6-m-high waves of ~ 20-min period flooded Vela

[1] Meteorological and Hydrological Service, Grič3, 10000 Split, Zagreb, Croatia. E-mail: kristian.horvath@cirus.dhz.hr
[2] Institute of Oceanography and Fisheries, Šetalište I. Meštrovića 63, 21000 Split, Croatia.
[3] Department of Geophysics, Faculty of Science, University of Zagreb, Horvatovac 95, 10000 Zagreb, Croatia.

Published online: 22 June 2018

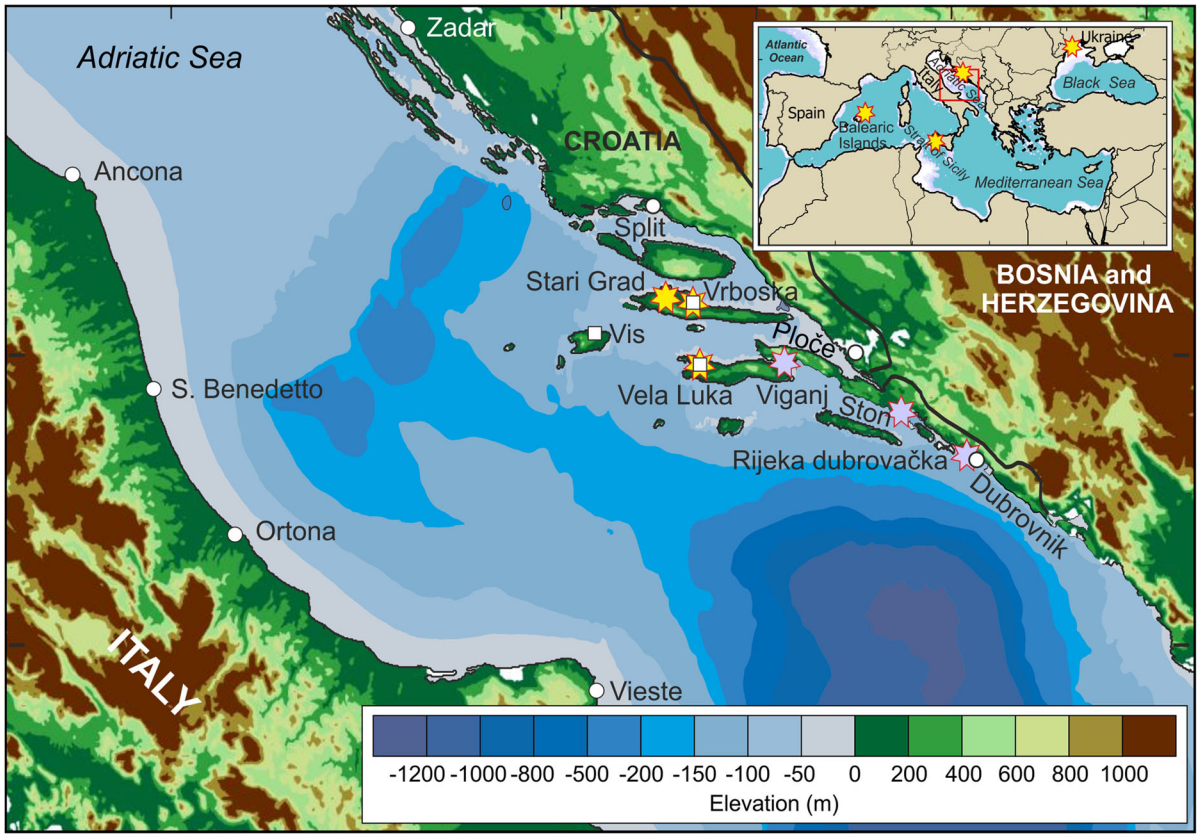

Figure 1
Area of interest. White squares indicate positions of air pressure stations and white circles of tide gauges. Stars mark locations hit by meteotsunami waves on 25 (yellow) and 26 (violet) June. Small inset shows wider Mediterranean area, with yellow stars pointing to locations of other Mediterranean and Black Sea meteotsunamis of 23–27 June 2014, and red box denoting area shown in the main plot

Luka repetitively for several hours, causing substantial damage and destruction (Orlić et al. 2010). An atmospheric pressure disturbance which propagated from the Apennine Peninsula in the southwest towards Croatian coast in the northeast was found responsible for the event. An attempt was made to reproduce this disturbance with an atmospheric numerical model (WRF) but to no avail: in spite the fact that various details of model setup were varied, the model failed to reproduce the pressure disturbance (Orlić et al. 2010).

Atmospheric gravity waves related to two other Adriatic meteotsunami were, however, reproduced by numerical atmospheric models: middle Adriatic meteotsunami of 27 June 2004 (Belušić et al. 2007), and the 1st meteotsunami of 22 August 2007 (Šepić et al. 2009). During the 2004 event, meteotsunamis hit Stari Grad and Mali Ston, a bay between mainland and Pelješac Peninsula (not shown), causing noticeable damage (Vilibić et al. 2004). It was shown by both observational data and non-hydrostatic MM5 atmospheric numerical model that this event was due to a single atmospheric gravity wave which propagated along the longer Adriatic Sea axis from the northwest towards southeast coupled to a convective cloud, in a so-called wave-CISK (conditional instability of the second kind) mechanism. Although atmospheric disturbance was reproduced, its exact shape, amplitude and timing were not exact. During the 2007 event, a 4-m-high meteotsunami hit Široka Bay on island of Ist in the northern Adriatic; observational data and non-hydrostatic WRF numerical model pointed that this meteotsunami was generated by a ducted atmospheric gravity wave which

propagated across the Adriatic Sea from the southwest towards the northeast. Again, simulation was not perfect; the entire reproduced pressure system was displaced about 40 km to the southeast when compared to measurements.

Numerical simulations of atmospheric conditions during meteotsunamis in other seas and oceans worldwide were, as well, partially successful in reproducing tsunamigenic pressure disturbances. Examples include 15 June 2006 event in Ciutadella Harbor, Menorca, Spain (Renault et al. 2011), 28 Oct 2008 event in Boothbay Harbor, Maine, USA (Vilibić et al. 2014) and 25 February 2009 event in Kyushu Island, Japan (Tanaka 2010). Either wave-CISK, ducted internal gravity waves or both phenomena acting in concert, were found responsible for meteotsunamis at these locations. However, the exact location, amplitude and lifecycle of tsunamigenic pressure disturbances remains challenging to simulate. This is due to small scales of the analyzed pressure disturbance and non-linearity of the atmospheric processes involved, as well as the need to simulate maintenance of pressure disturbance over several cycles, which often requires a fine balance between generation and dissipation of those events in numerical models. At typical length scales of pressure perturbations causing meteotsunamis (10–50 km), state-of-the-art numerical simulations need to be used at grid spacings of around 1 km at the most to avoid excessive numerical diffusion (Horvath and Vilibić 2014). For this reason, challenging sub-kilometer grid spacing simulations should be considered for simulation of meteotsunamis.

What diverges the 2014 event from the other known events is a multitude of individual atmospheric pressure disturbances and accompanying multitude of individual meteotsunami waves. It appears that very peculiar conditions, which existed in the atmosphere during days in question, supported continuous generation of small but intense atmospheric pressure disturbances (Šepić et al. 2015). Moreover, the Adriatic multi-meteotsunami event was not isolated, but rather, a link in a chain of meteotsunami events which hit the Mediterranean and Black Sea regions during 23–27 June 2014. Besides for the Adriatic, strong meteotsunamis appeared at several other locations. First to be affected was Ciutadella harbor on Menorca Island (Spain), where 1-m-high waves were observed during night hours of 22/23 June. Then, in the late afternoon hours of 25 June, strong and destructive 1-m-high tidal bore was filmed propagating through Mazara river (Mazara del Vallo, Sicily, Italy) (Šepić et al. 2018b). Finally, in the morning hours of 27 June, a few beaches in Odessa (Ukraine) were hit by a sudden tsunami-like wave of a 2 m height, injuring five persons and causing a widespread panic (Šepić et al. 2018a). All of these events occurred while a particular tsunamigenic synoptic situation was present over respective areas. Analysis of the atmospheric processes conducive for the Adriatic meteotsunamis can, therefore, also shed light onto meteotsunami-generating processes over other regions of the Mediterranean as well.

In Sect. 2, we present data and methods used for investigation of the event. Sections 3 and 4 present results of discussion of observational and numerical analysis, respectively, while Sect. 5 concludes the findings of the study.

2. *Data and Methods*

2.1. *Observational Data*

Air pressure was measured at three high-resolution (1 s sampling interval) high-precision (accuracy of ± 0.01 hPa) stations with Väisälä PTB330 pressure sensor: Vis, Vrboska and Vela Luka (Fig. 1); 1 min time averages of pressure data were used for model verification. Sea level was measured with resolution of 1 min and accuracy of ± 1 mm with OTT Thalimedes instrument at three coastal stations: Split, Ploče and Dubrovnik. For visualization purposes, all measured data were filtered with a 6-h Kaiser–Bessel high-pass filter (Thomson and Emery 2014). In addition, prior to filtering, sea-level data were de-tided with the use of T-TIDE software (Pawlowicz et al. 2002).

For the determination of the synoptic conditions and key vertical characteristics of atmosphere, surface and upper synoptic maps were used (available at http://www1.wetter3.de/). We have also used remote sensing data, in particular maps of lightning data and

composite of Meteosat-MSG infrared satellite imagery overlaid with a precipitation and aforementioned lightening data (source https://www.lightningmaps.org).

2.2. Modeling Methodology

The modeling tool employed for this study was the non-hydrostatic Weather Research and Forecasting model (WRF-ARW, V3, Skamarock et al. 2008). The WRF model solves the fully compressible, non-hydrostatic equations of motion in an Arakawa-C grid. For the purpose of more accurate numerical computation in the model, the thermodynamic variables are written in perturbation form for all three components of wind, potential temperature, geopotential, air pressure and scalars such as turbulent kinetic energy (TKE) and mixing ratio for different phases of water vapor.

The information about general configuration of model run is given in Table 1. Here, two-way nesting was used in the interaction of four domains with different grid spacing; from 13.5 km in the largest domain covering central Mediterranean (A in Fig. 2), 4.5 km in domain B, 1.5 km in domain C and up to 0.5 km horizontal grid spacing in the innermost domain D (Fig. 2) which includes part of the southern Adriatic Sea and several islands (i.e. Hvar and Korčula). Domains were optimized to represent: (1) basic driving forces that affect the appearance of meteotsunami, (2) the inflow/outflow wind relationship, (3) important topographic features and (4) area of interest (i.e. central-eastern Adriatic). It should be noted that the use of sub-kilometer domains in atmospheric simulations requires an extra attention related to potential double-counting of turbulent eddies in resolved and parametrized parts of model solutions (Horvath et al. 2012) and is, therefore, case dependent. Our choice for the setup in this case is justified since meteotsunami occurred during the morning hours and in a cloud zone when and where atmospheric boundary layer was not deep enough to support double-counting. In the largest domain, the mountain range of Alps and the Apennines were included to capture the major synoptic forcing. Defined over the middle and south Adriatic region, the third 1.5-km grid-spaced domain (C in Fig. 2) has been included as well and nested within the larger second (dx = 4.5 km, B in Fig. 2) domain. In vertical, grid consists of unequally set 81 sigma levels. They follow terrain up to upper limit defined by 70 hPa-constant pressure level. The lowermost 2 km

Table 1

Summary of numerical setup in WRF model

Domains	4 (A–D), two-way nested	
	Grid points	Resolution
Domain A	160 × 133	13.5 km × 13.5 km
Domain B	133 × 133	4.5 km × 4.5 km
Domain C	184 × 184	1.5 km
Domain D	142 × 151	0.5 km × 0.5 km
Vertical grid (terrain-following coordinate)	81 levels (the lowest half-sigma level ∼ 10 m)	
	Top of the model = 70 hPa	
Topography and land use	30′ USGS data	
Initial/boundary conditions	Analysis from the ECMWF at 0.125°	
Parametrizations		
Microphysics	Morrison 2 moment scheme (Morrison et al. 2005)	
Cumulus parameterization	Kain-Fritsch scheme (Kain 2004) only in Domain A	
Long-wave radiation	RRTM scheme (Mlawer et al. 1997)	
Short-wave radiation	Dudhia scheme (Dudhia 1989)	
Turbulence scheme	MYJ scheme (Janjić 1994)	
Surface layer	Eta scheme (Janjić 1994)	
Soil temperature	Five-layer thermal diffusion scheme (Dudhia 1996)	

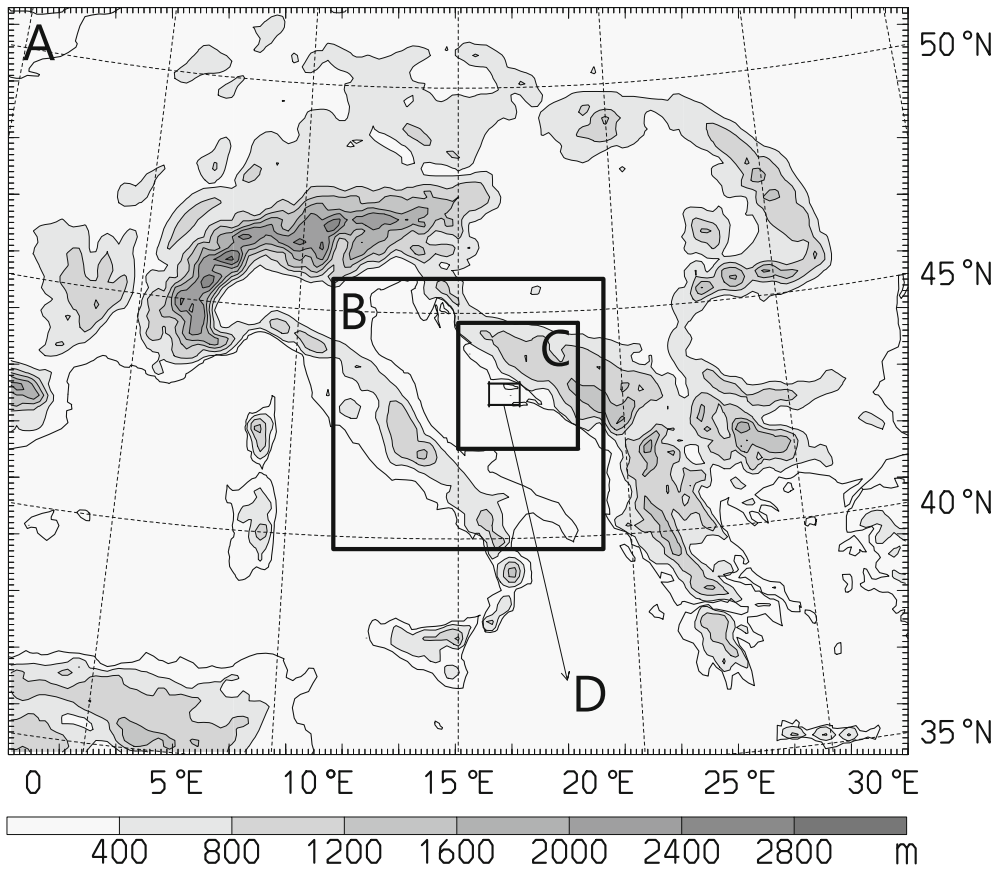

Figure 2
Computational domains and topography (grid A) for the WRF model run

of the atmosphere are resolved by 17 levels and the lowest half-sigma level is set to ∼ 10 m above surface.

The model is optimized with main physical parameterizations of WRF (Table 1) in defining calculations of turbulence, soil characteristics, radiation, microphysics, etc. similar to Kehler-Poljak et al. (2017). Therefore, the local Mellor–Yamada–Janjić (MYJ) scheme is applied for the atmospheric boundary layer (Janjić 1994) in combination with an Eta surface-layer scheme and a five-layer thermal diffusion scheme (Dudhia 1996) for soil temperature. Radiation is calculated through the use of a rapid radiative-transfer model (RRTM) scheme (Mlawer et al. 1997) and a Dudhia scheme (Dudhia 1989) for the long-wave and short-wave radiation, respectively. For microphysics, a Morrison 2 moment scheme was chosen which predicts the mixing ratio of different hydrometeor species (Morrison et al. 2005). Taking into account dependence between the use of cumulus parameterization and grid spacing, we only applied Kain–Fritsch scheme (Kain 2004) in the largest domain.

Topography and land use in the model were obtained from the US Geological Survey's 24-category data set at a 30″ resolution. Initial and boundary conditions were supplied to the 13.5-km grid from 6-h operational analyses data of European Centre for Medium Range Weather Forecasts (ECMWF) at 0.125° × 0.125° grid. The numerical simulation started on 24 June 2014 at 12:00 UTC and was set to run for next 2.5 days considering the first 12 h as a spin-up time.

3. Observational Analysis

3.1. Air Pressure and Sea-Level Station Data

Original and high-pass (6-h Kaiser–Bessel filter) filtered sea-level time series from three middle Adriatic tide gauges are shown in Fig. 3. In spite of the fact that no strong meteotsunamis were observed at these particular locations, tide gauges still recorded intensification of high-frequency sea-level activity. Oscillations are best seen in Ploče records, where they started with an arrival of a wave crest (∼ 30 cm) at 05:34 UTC. Oscillations remained intensified through most of 25 June, calmed down during night of 25/26 June, and then again increased during morning hours of 26 June, in agreement with observed meteotsunami events.

Air pressure time series show similar strengthening of high-frequency activity during morning hours of 25 June (Fig. 4), concurrent with arrival of a longer period low which was present over the middle Adriatic throughout 25 June 2014. High-frequency oscillations started around 04:40 UTC with a pronounced air pressure disturbance of 100–120-min duration and 3.2 hPa peak to trough height. Šepić et al. (2016) estimated velocity of this disturbance to 27 m/s and 250°. Two shorter periods (up to 30 min), but higher intensity (rate of air pressure change up to 2.4 hPa/5 min and 0.7 hPa/min) air pressure disturbances followed. These ones propagated faster, and their velocity was estimated to 40 m/s and 272°. Next, followed a series of high-frequency oscillations of very short period [O(5–10 min)] which persisted throughout morning and afternoon hours of 25 June. Velocity of these disturbances was determined to be 45 m/s and 223°. Oscillations calmed down during night hours of 25/26 June, just to strengthen again during morning of 26 June. Oscillations of 26 June

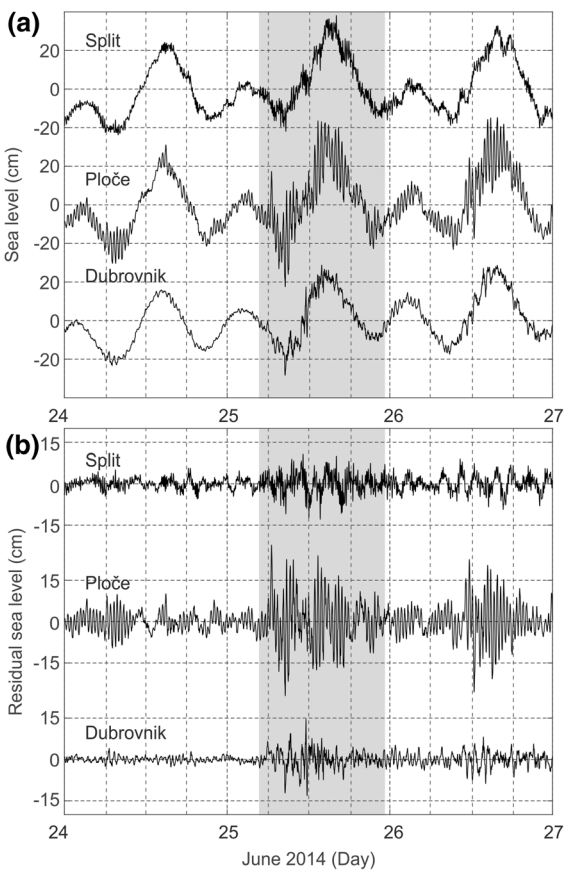

Figure 3
Time series of **a** sea-level data, **b** de-tided and high-pass filtered (6-h Kaiser–Bessel filter) sea-level data measured in the target area

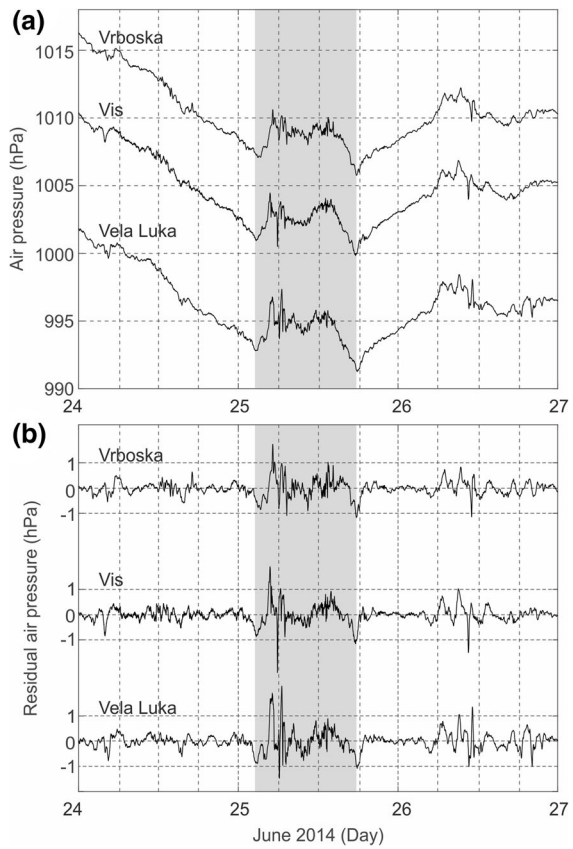

Figure 4
Time series of **a** air pressure data, **b** high-pass filtered (6-h Kaiser–Bessel filter) air pressure data measured in the target area

were of 30–40 min, and had a maximum peak to trough height of 2.0 hPa. Estimated velocity was 30 m/s and 211°.

3.2. Synoptic Analysis

Model initialization started on 24 June 2014 at 12:00 UTC when a large deep cyclonic vortex positioned over North Europe moved slowly eastward (Fig. 5). This low-pressure formation existed during the whole investigated period and was associated with formation of a large frontal structure located northward of the area of interest. Still, this slowly eastward-moving frontal system itself had no significant influence on the southern part of the Adriatic. At the same time, over the Mediterranean, two opposite synoptic formations were observed (Fig. 5a). A low-pressure area, which existed in the middle and lower half of the atmosphere, was centered over the Iberian Peninsula, while over the southern Mediterranean a high-pressure ridge aloft marked weather conditions.

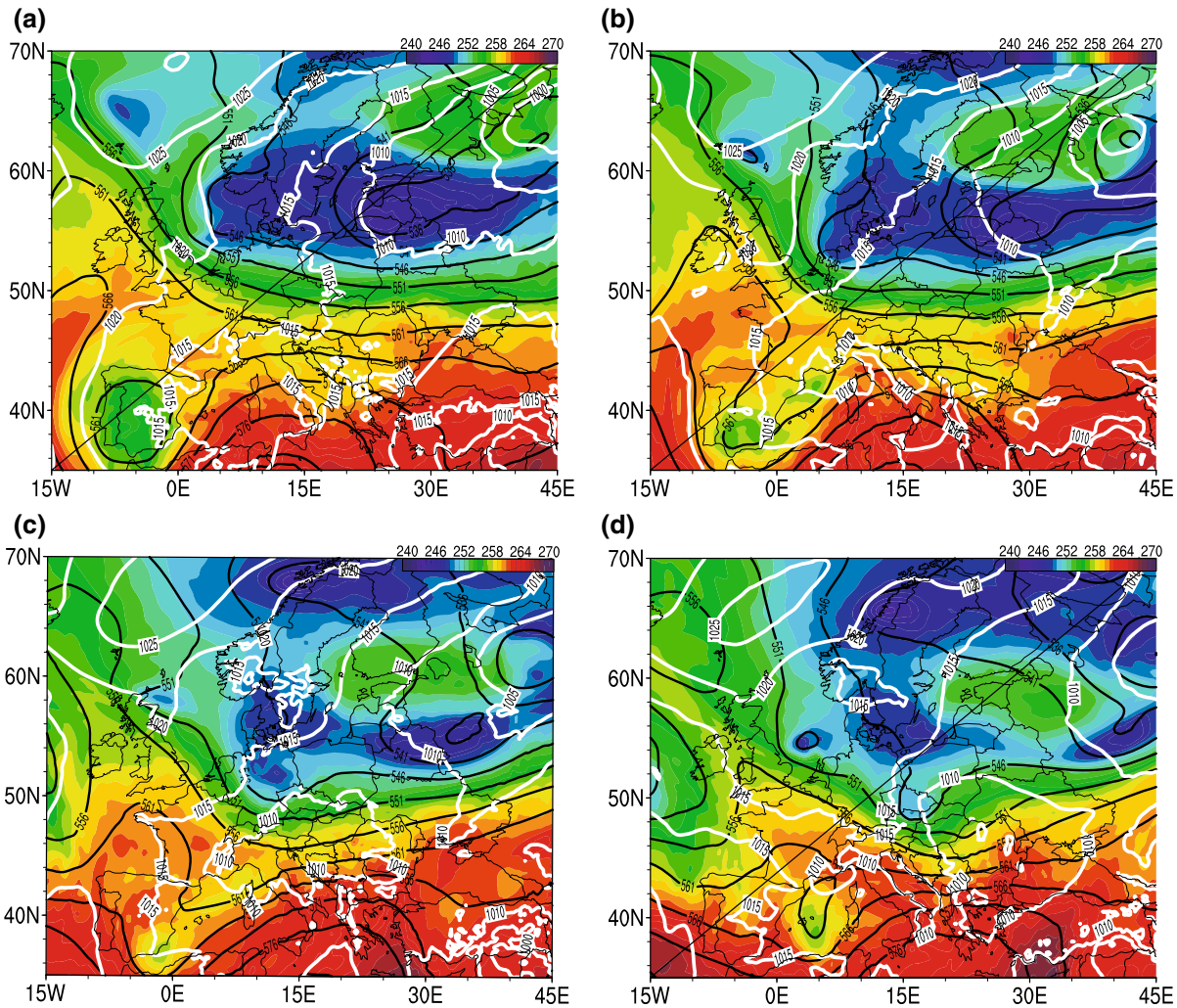

Figure 5
Synoptic settings on 24–26 June 2014 from ECMWF analysis—a mosaic of geopotential height (gpdam, black contours) and temperature (K, shaded areas with legend in the upper right corner) at 500 hPa and surface pressure (hPa, white contours) for: **a** 24/06 12:00 UTC, **b** 25/06 00:00 UTC, **c** 25/06 12:00 UTC and **d** 26/06 12:00 UTC

Because of such pressure distribution, in the area of transition between the northern low and the southern high baric formations, a significant pressure gradient was formed. It contributed to strengthening of the mostly southwesterly (SW) wind aloft (i.e. layer 700–500 hPa) on the back side of the ridge above the Apennines and Adriatic with wind speeds in the range of 20–35 m/s. The SW wind was the dominant feature of the middle atmosphere during the whole simulation.

Described upper large-scale pressure conditions resulted in the Alpine cyclogenesis which influenced surface pressure distribution (Fig. 5b). Over the western Mediterranean and the northern Italy, in the lowermost layer, a shallow eastward-moving low-pressure system developed during the following days. The pressure system was modified after the passage over the Apennine peninsula, which caused the separation of the flow and perturbations in the pressure field over the Adriatic. The result was the occurrence of two separate centers of cyclones on both sides of the peninsula: (1) mesocyclone over the Adriatic in the hinterland of Apennines and (2) the Genova cyclone. The Genoa system continued to develop and intensify in time (Fig. 5c) gradually forming one large pressure system characterized by a local instability zone. Observed local instability had an effect on the daytime occurrence of convection in the area of interest (on 25 June). Towards the end of 26 June, the low-pressure structure leaved the area of interest and moved eastward while in Genova Bay a new low-pressure system formed (on 26 June, Fig. 5d).

Described mean surface pressure distribution generated mostly southeasterly (SE) near-surface winds on the northern part of the Adriatic and along the eastern Adriatic coast on 25 June. In the nighttime hours on 26 June, a northwesterly wind shortly appeared in the northern Adriatic while SE wind prevailed southward (i.e. along the eastern Adriatic coast) and further during the daytime. Near-surface winds reached moderate speeds of 10 m/s.

3.3. *Convection and Clouds*

In hours preceding meteotsunami, remote sensing indicated that precipitation and lightning occurred in the central Adriatic. A more detailed inspection of lightning records in 6 h prior and after the meteotsunami event suggests that lightning was continuously present in the area and that precipitation was at least partially of convective origin (Fig. 6a). Further analysis shows, however, a weak lightning activity (just a few strokes recorded southeast of Vela Luka) in the Vela Luka area in a 1-h interval preceding meteotsunami (from 05:30 to 06:30 UTC) suggesting that deep convection was not very active just prior to the meteotsunami event (Fig. 6b) apart from a few isolated convective cells. This does not eliminate deep convection as a potential cause of the meteotsunami because first, meteotsunamis can be caused by deep convection farther away from the hit location (Šepić et al. 2018a). Second, wave-CISK theoretical model applies to interplay of isolated convective cell and gravity waves and, therefore, isolated convective cells may also have potential to cause meteotsunamis.

Furthermore, at 06:00 UTC satellite imagery of visible spectra showed wave-like cloud structures (Fig. 6b) and similar structure was found in satellite estimates of precipitation (not shown). As inferred by a lack of lightning in the area of wave-like precipitation pattern, it appears that the convective character of this pattern was not very intense. Wavelengths range from scales of 20–40 km right over the Apennines. However, over the Adriatic cloud structures of similar wavelengths were not clearly visible, but rather suggested less intensive cloud structures of longer wavelengths. These structures and their wavelengths suggest that these waves might be mountain-induced or mountain-enhanced gravity waves.

To cause a meteotsunami, wavelengths of pressure oscillations required for Proudman resonance should be several times less than propagation path of pressure oscillation over the sea (Vilibić 2008), implying that over the Adriatic most favorable wavelengths would be < 50 km. Therefore, it is evident that wavelengths found over the Apennines (20–40 km) correspond to wavelengths that could cause a meteotsunami in the Adriatic. While those cloud structures of scales 20–40 km are not visible on satellite imagery over the Adriatic, their existence cannot be discarded based on our analysis because

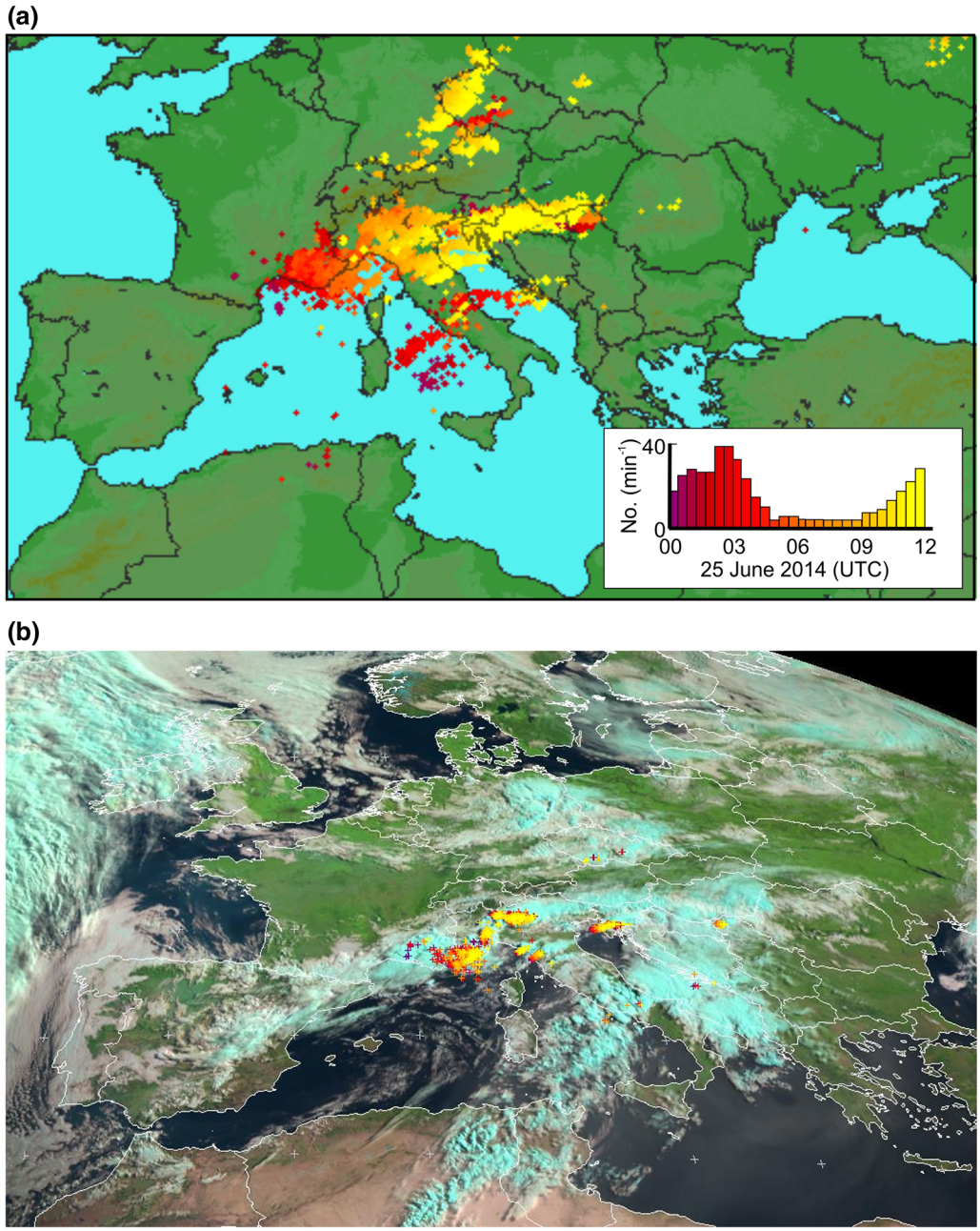

Figure 6
a Accumulated 12-h lightning data at 12:00 UTC 25 June 2014 (source: http://www.lightningmaps.org) and **b** composite of EUMETSAT MSG visible spectra satellite imagery with lightning in preceding hour at 06:00 UTC 25 June 2014 (source https://www.lightningmaps.org)

they could be masked by other types of clouds in the atmosphere or could be too dry/wet to be clearly identified. Therefore, it can be concluded that some convection did occur in the region and that atmospheric properties were generally conducive to wave-like organization of clouds which was modulated by the Apennine mountain range. Similar conclusions related to other Adriatic meteotsunamis were previously reached using satellite imageries (Belušic and Strelec-Mahovic 2009). Furthermore, it may be noted

that the presence of moderate convection was found in some other meteotsunamis such as the Boothbay harbor event where moderate convection was organized in a wave-like structure of similar wavelengths and coexisted with smaller scale internal gravity waves (Vilibić et al. 2014, Horvath and Vilibić 2014).

4. Numerical Analysis

4.1. Model Evaluation

Analysis of measured data in Sect. 3 suggests major meteotsunami event occurred in Vela Luka, Croatia, around 06:30 UTC. This event was followed by three other events: in Rijeka Dubrovačka at approximately 11:00 UTC, Stari Grad at around 13:00 UTC, and Vrboska at approximately 15:00 UTC. The strongest recorded pressure oscillations reached amplitude of approximately 4 hPa with rates of pressure change of up to 2.4 hPa/5 min and 0.7 hPa/min.

Measured and simulated time series of mean sea-level pressure in Vela Luka are shown in Fig. 7. For this comparison, we used output from sub-kilometer domain D (0.5 km grid spacing). For both simulated and measured data, 1-min averages of sampled 1-s data are plotted. The mesoscale pressure pattern of the entire day of 25 June 2014 is well simulated including diurnal variability of mean sea-level pressure (MSLP) which shows maximal values in the morning (1012 hPa) and minimal values in the afternoon (1006 hPa). Even more, the period of the highest mean sea-level pressure oscillations in Vela Luka recorded between 05:00 and 14:00 UTC 25 June 2014 is well reproduced in the model simulation, despite a time shift of model solution of approximately 1 h compared to measured data and a noticeable overestimation of duration of the surface pressure perturbations.

The strongest MSLP oscillations are simulated around 06:00 UTC 25 June 2014 and yield maximal rate of pressure change of approximately 1.4 hPa/min (domain D), and were thus comparable to measurements with recorded pressure tendency of 0.7 hPa/min. The difference might easily be due to temporal and spatial errors typical for point-based verification

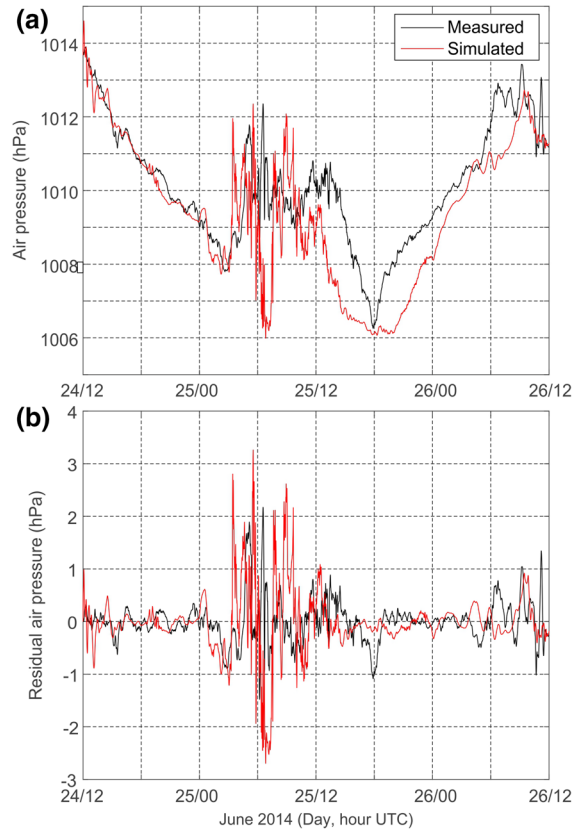

Figure 7
Time series of **a** measured and simulated MSLP, **b** high-pass filtered (6-h Kaiser–Bessel filter) measured and simulated MSLP for Vela Luka station on 12 UTC 24 June 2014–12 UTC 26 June 2014

of the models. Within the period of MSLP oscillations, measurements revealed two distinct MSLP maxima which were preceded and followed by MSLP minima. Such a structure is simulated as well, although the exact number and timing of maximal and minimal values is not fully reproduced. Wavelet plots of measured and simulated high-pass (6-h Kaiser–Bessel filter) MSLP time series are shown in Fig. 8. We focus on high-pass series, as tsunamigenic air pressure disturbances primarily occur over higher frequencies (i.e. for $T < 6$ h). We can notice that simulated time series reproduce onset time and general energetic structure of measured series quite successfully. There are, however, some differences. Simulated disturbances are of longer duration, they are more energetic and, when most energetic, cover wider range of periods (from 5 towards 250 min) than

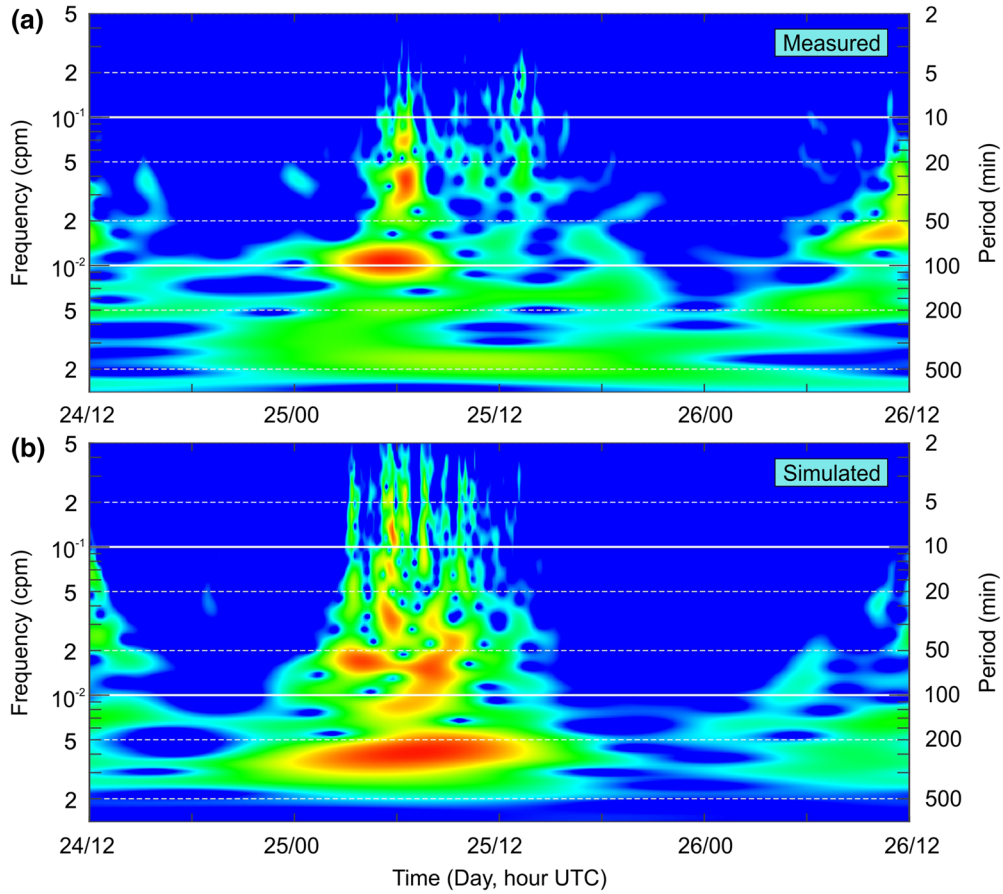

Figure 8
Wavelets of: **a** measured MSLP, **b** simulated MSLP, all for Vela Luka station. Wavelets are estimated for high-pass-filtered time series (6-h Kaiser–Bessel filter)

measured ones. Oppositely, measured series are less energetic, of shorter duration, and when most energetic, they appear at distinct periods of 100, 25–33 and 15 min.

Since observed MSLP oscillations were likely due to propagating ducted internal gravity wave package or convection, it is not likely that model may be able to reproduce precise details of these oscillations. Nevertheless, model simulation represents MSLP oscillations quite well and will be used for analysis of mesoscale structure of the atmosphere and environment conducive to the occurrence of this meteotsunami event.

4.2. Surface Pressure and Wind Distribution

Simulated mean sea-level pressure and surface winds around the time of meteotsunami are shown in Fig. 9. At 05:00 UTC 25 June 2014, pressure oscillations were evident in the wider central Adriatic target area. West of the Vela Luka harbor, modeled mean sea-level pressure field showed a primary pressure perturbation pattern with several maxima and minima yielding a maximum of pressure drop/rise of 6 hPa over a $\sim$ 25 km distance. Similar, albeit not so intensive, pressure gradients were found in other areas in the vicinity. The largest pressure disturbances were accompanied with a surface wind field curl and wind intensification. Some of simulated pressure perturbations were found south of Vela Luka and were of smaller scales when compared to the

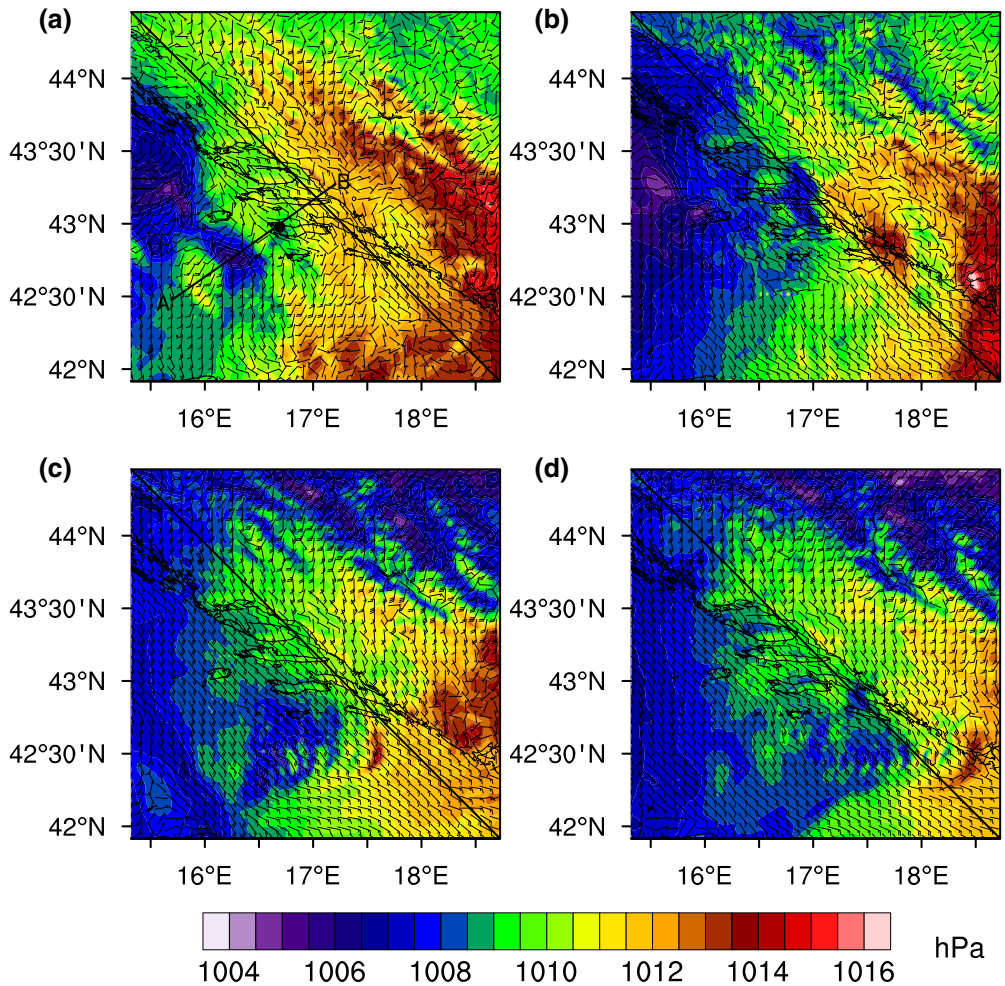

Figure 9
Simulated MSLP (hPa) and 10-m wind barbs (kt) from WRF domain C at 05:00 UTC, **b** 06:00 UTC 25 June 2014, **c** 11:00 UTC 25 June 2014 and **d** 12:00 UTC 25 June 2014. Cross section AB is used in Figs. 14, 15 and 16. Vela Luka is denoted with a filled black circle in panel **a**

primary pressure perturbation pattern. During following minutes, the primary pressure perturbation moved over Vela Luka area. One hour later, at 06 UTC 25 June 2014, pressure perturbations were found further eastward, close to the mainland coast, with several small-scale pressure perturbations, accompanied by a small-scale wind perturbations, still present in the Vela Luka area and surrounding region.

A few hours later, between 10:00 and 11:00 UTC 25 June 2014, intense internal gravity waves were simulated to propagate south of Vela Luka towards the eastern Adriatic coast. Mean sea-level pressure oscillations reached as high as 5 hPa in a range of individual peaks and troughs of the gravity wave packet. The group velocity of the internal gravity wave packet is estimated to $\sim$ 28 m/s, which is within range of velocities determined from measured data. As for wind, wind field appears to be rather uniform over the area, with surface winds dominantly of southeasterly direction.

Propagation of this secondary pressure disturbance pattern towards the eastern Adriatic coast is in an excellent agreement with observed meteotsunami event in Rijeka Dubrovačka. Precisely at the time when simulated wave packet reached the area of Rijeka Dubrovačka, meteotsunami event occurred.

Simulated pressure disturbances have characteristics conducive for generation of meteotsunamis:

rates of air pressure change (> 1 hPa/min), dimensions (~ 25 km) propagation speed (~ 28 m/s) and direction (towards endangered area) of these disturbances, all fall within ranges which are favorable for meteotsunami generation over the middle Adriatic area (Vilibić et al. 2004; Orlić et al. 2010; Šepić et al. 2016). Oppositely, simulated winds, with domain D average wind at 05 UTC yields 5.0 m/s, with very localized maximum of wind speed of 10.5 m/s, are of insufficient strength to generate meteotsunami waves. In their modeling studies, Orlić et al. (2010) and Šepic et al. (2015) show that sustained winds of ~ 10 m/s speeds are ineffective in generating significant long ocean waves over sea depths > 10 m. Since, sea depths over the middle Adriatic drop to more than 50 m very close to the coast (Fig. 1), we can conclude that wind did not contribute significantly to generation of the middle Adriatic meteotsunami event of 25 June 2014.

A sheer number of simulated atmospheric waves suggest that the atmosphere was generally conducive to internal gravity waves, which are one of the two most common causes of meteotsunamis (e.g. Monserrat et al. 2006; Vilibić et al. 2004).

An even more detailed structure of the pressure perturbations around Vela Luka can be studied using results of domain D, where pressure perturbations were simulated with 0.5 km horizontal grid spacing (Fig. 10). At 05:00 UTC, an area of high pressure was located just west of Vela Luka harbor with maximum reaching nearly 1012 hPa. Further to the southwest, pressure minima reached as low as 1006 hPa. This pressure dipole travelled from ESE to ENE. Distance between crest and ridge of that system was approximately 25 km, in agreement with results from domain C. This wavelength is in accordance with wavelengths of cloud structures over the Apennines, as estimated from the satellite imagery (Sect. 3.3). Further to the south and southeast several shorter oscillations in the mean sea-level pressure were simulated as well with amplitudes of up to 2 hPa.

At 06:00 UTC, just prior to the meteotsunami, the main pressure oscillation packet moved towards ENE with its amplitude somewhat decayed due to dissipation. It can be estimated that system travelled at a propagation speed of approximately 20 m/s, which is somewhat below propagation speed inferred by analysis of measurements. In the area around Vela Luka, other smaller scale pressure perturbations propagated from west to east. Those pressure perturbations were not so intensive as the main pressure oscillation packet.

The above analysis of mean sea-level perturbations as well as results of verification presented in the preceding subsection demonstrate that model simulations successfully reproduced pressure oscillations which caused middle Adriatic meteotsunami events. Next, we proceed with analysis of atmospheric structure during the event and analyze in more detail which atmospheric processes were collocated with the mean sea-level pressure oscillations and were the cause of surface pressure perturbations.

4.3. Convection and Gravity Waves

Simulated hourly precipitation shows that precipitation in Vela Luka started around 05:00 UTC 25 June 2014, when precipitation zone moving eastward reached Vela Luka (Fig. 11). In the next hour, until 06:00 UTC 25 June 2014, precipitation zone moved over Vela Luka. Approximately, 4 mm of precipitation was simulated over Vela Luka within an hour, with somewhat more precipitation south of Vela Luka. Since 2 mm of precipitation was recorded at ground station in Vela Luka, model was relatively successful in simulating measured moderate precipitation amounts. Precipitation pattern extends and stretches towards the east, suggesting precipitation was caused by convective cells propagating from the Apennines towards the eastern Adriatic coast.

Convection and internal gravity waves suggest the presence of vertical velocity perturbations. On 05:00 UTC 25 June 2014, vertical velocity in mid-troposphere (at 3 km AGL) confirms that area around Vela Luka was conducive to vertical air displacements (Fig. 12). Shape of perturbations corresponds to both convection and internal gravity wave packets. Horizontal scale of vertical velocity perturbations is similar to horizontal scale of MSLP perturbations, ranging from 20 to 40 km. Such perturbation wavelengths correspond to wavelengths that may react with the sea surface through Proudman resonance over the Adriatic (Vilibić 2008). At 06:00 UTC 25 June 2015, the area of the most intensive vertical

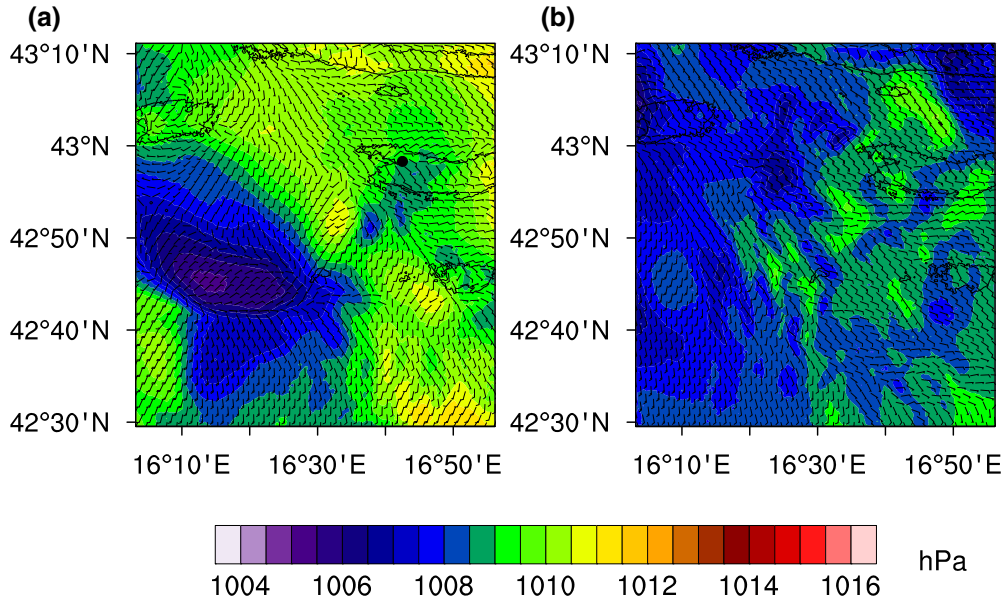

Figure 10
Simulated MSLP (hPa) and 10-m wind barbs (kt) from WRF domain D at **a** 05:00 UTC 25 June 2014 and **b** 06:00 UTC 25 June 2014

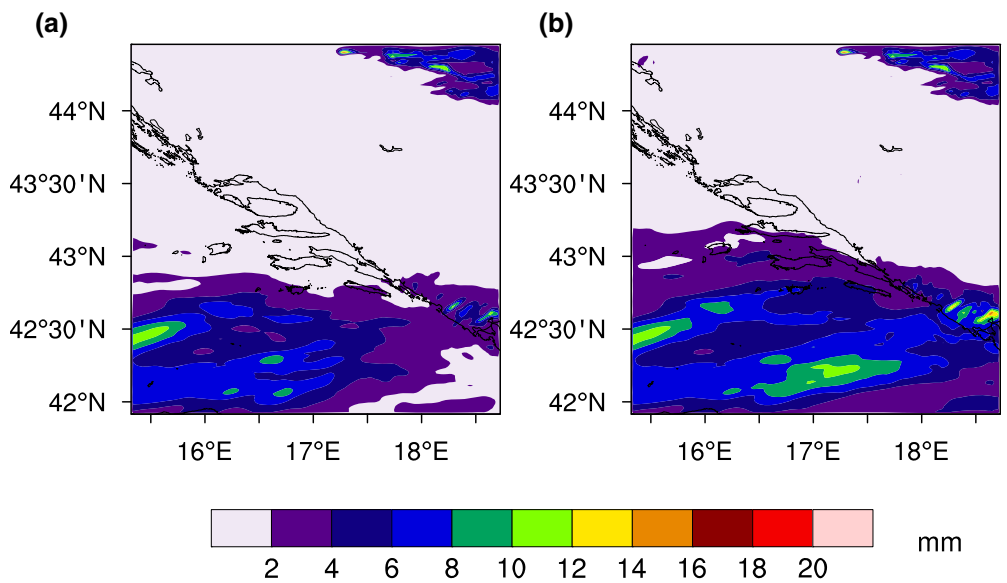

Figure 11
Simulated hourly precipitation at **a** 05:00 UTC 25 June 2014 and **b** 06:00 UTC 25 June 2014 from model domain C

velocity perturbations moved towards ENE, crossing the Vela Luka area. At 11:00 UTC another gravity wave packet approached the area and moved towards the eastern Adriatic coast (Fig. 13). The wave packet existed already at 10:00 UTC (not shown) and persisted even after 12:00 UTC when it reached the coastline and caused a meteotsunami in the Rijeka Dubrovačka area. Phase speed of that internal gravity wave package was around 30 m/s which corresponds to estimates from surface measurements. This

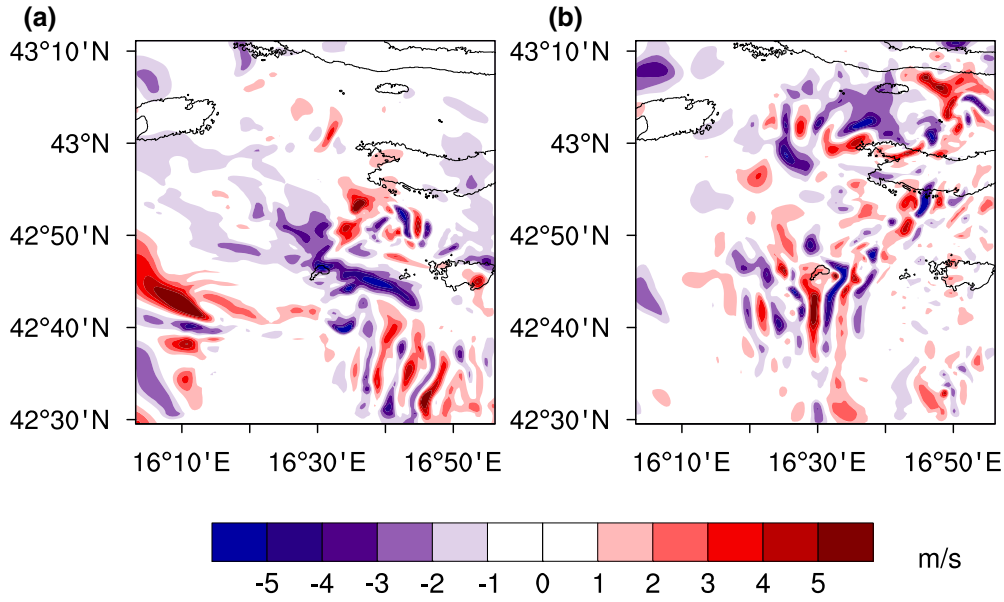

Figure 12
Simulated vertical velocity at 3 km AGL at **a** 05:00 UTC and **b** 06:00 UTC 25 June 2014 from domain D

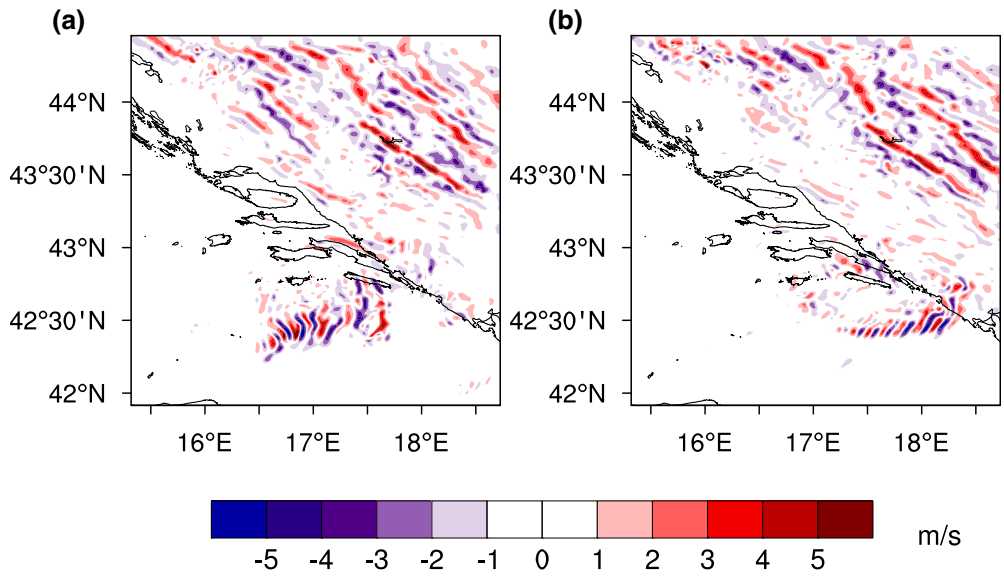

Figure 13
Simulated vertical velocity at 3 km AGL at **a** 11:00 UTC and **b** 12:00 UTC 25 June 2014 from domain D

suggests a clear and consistent relation between MSLP perturbations and mid-tropospheric activity, as evidenced by vertical velocity perturbations. The vertical structure of the atmosphere is analyzed in more detail in the next section.

4.4. Vertical Structure of the Atmosphere

Vertical structure of the atmosphere is analyzed around the time pressure perturbations moved over Vela Luka area. We focus on two phenomena, wave-CISK and wave duct, that can maintain pressure

perturbations over a sufficiently (e.g. several cycles) long time for atmospheric pressure disturbance to couple with sea level. Wave-CISK presents the coupling between a gravity wave and convection, found typically in tropics, where the associated convergence forces the moist convection, and convective heating provides the energy for the wave (Lindzen1974). Wave duct occurs when a stable lower troposphere is overtopped with a sheared unstable layer in mid-troposphere which reflects the energy of the internal gravity wave towards the surface and therefore ducts internal gravity waves over long distances (Lindzen and Tung 1976; Lin 2007).

Vertical cross section of the potential temperature and vertical velocity at 05:00 UTC 24 June 2014 (Fig. 14) suggests that moderate potential temperature and vertical velocity perturbations were present just west of Vela Luka. East of Vela Luka perturbations were much weaker or inexistent in some areas. These perturbations west of Vela Luka bay were slightly tilted with height in the mid- and upper troposphere and collocated with a moving precipitation zone. This suggests that a mechanism resembling wave-CISK was at play to maintain the pressure perturbations over a certain period of time. In the following hour, the area of the most intense perturbations moved eastward crossing Vela Luka area and slowly dissipated. As seen earlier, at 11:00 UTC 24 June 2014 another wave packet moved over the area south of Vela Luka and propagated towards the Adriatic coast. This wave packet corresponds to MSLP oscillations at the sea surface that affected Rijeka Dubrovačka.

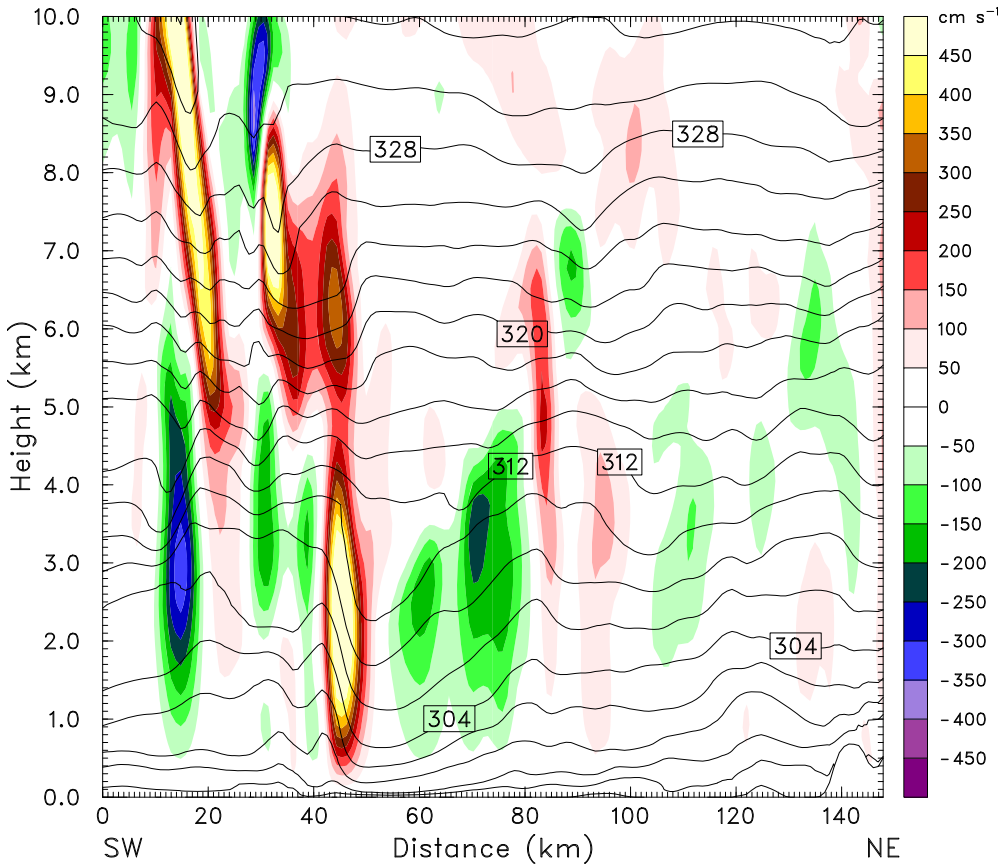

Figure 14
Vertical cross section of simulated potential temperature (solid black contours) and vertical velocity (shaded) over Vela Luka area 05:00 UTC 25 June 2014. Cross section is denoted in Fig. 9

During propagation of the pressure perturbations and disturbance aloft, the low-level atmosphere was statically stable providing a layer where perturbations can be maintained due to gravity acting as restoring force (Fig. 15). The same structure of the atmosphere was maintained in the next hours and also during the lifecycle of secondary pressure perturbations, which affected Rijeka Dubrovačka. Therefore, we analyze the presence of environmental conditions required for a wave duct. A duct can occur when the following conditions are satisfied: (1) a stable layer of air in which the waves can propagate is near the ground, (2) this stable layer is topped by a sheared unstable layer with Richardson number $R_i < 0.25$, (3) there is an embedded critical level in the unstable layer aloft, and (4) the depth of the wave duct D is $D = l_z\ (1/4 + 1/2n)$, where l_z is the vertical wavelength and $n = 1, 2$, etc.

The depth of the stable layer was from 3 to 4 km AGL and it was topped with a limited area of unstable layer aloft. This area was above and around the location of the surface pressure and mid-tropospheric perturbations. In the unstable layer, environmental Richardson number was below 0.25 suggesting dynamically unstable environmental conditions. An existence of local Richardson number minimum of less than 0.25 was also found at height from 2.5 to 3 km AGL. Therefore, in the region around the propagating perturbations conditions (1) and (2) are satisfied.

The existence of the critical level in the unstable air aloft is a crucial condition required for trapping of the energy below. In case of, e.g. internal

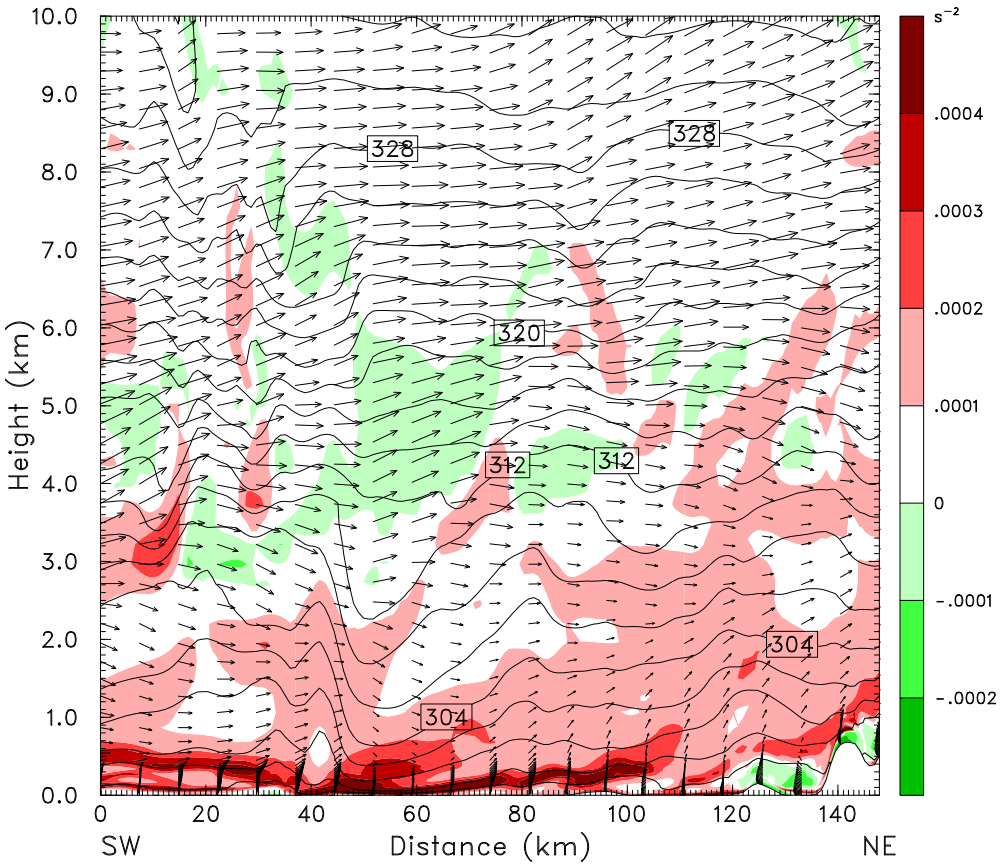

Figure 15
Vertical cross section of simulated potential temperature (solid black contours) and moist Brunt–Väisälä frequency (shaded) and horizontal wind vectors at 05:00 UTC 25 June 2014. Cross section is denoted in Fig. 9

gravity waves, this layer acts as a reflection or over-reflection layer for the energy of the waves (Lin 2007). In this case, a critical level would be a level where the wind component in the direction of the environmental flow is the same as the speed of propagating disturbances. As seen earlier, the latter was estimated from measurements to be between 27 and 40 m/s. As seen in Fig. 16, wind component in the direction of the flow which equals 30 m/s (108 km/h) was found in and near the unstable layer which is, concerning simulation uncertainties, very near to satisfy the given criterion for a duct. Finally, a rough estimate of the depth of a duct can be made using simulated average values of Brunt–Vaisala frequency N (0.01 s^{-1}), mean wind speed U near the top of the stable layer (22.5 ms^{-1}) and phase speed of internal gravity waves c_p (30 ms^{-1}) and approximating vertical wavelength $k_z = 2\pi \times (c_p - U)/N$, which yields $k_z = 4.7$ km and $D = 3.5$ km. This value corresponds to simulated depth of the stable lower tropospheric layer. Similar values were found in the case of Boothbay event (Vilibić et al. 2014).

The existence of the critical level in the unstable layer was maintained in the next hours and present during the lifecycle of the secondary pressure perturbations that affected Rijeka Dubrovačka, thus in hours when internal gravity wave packet

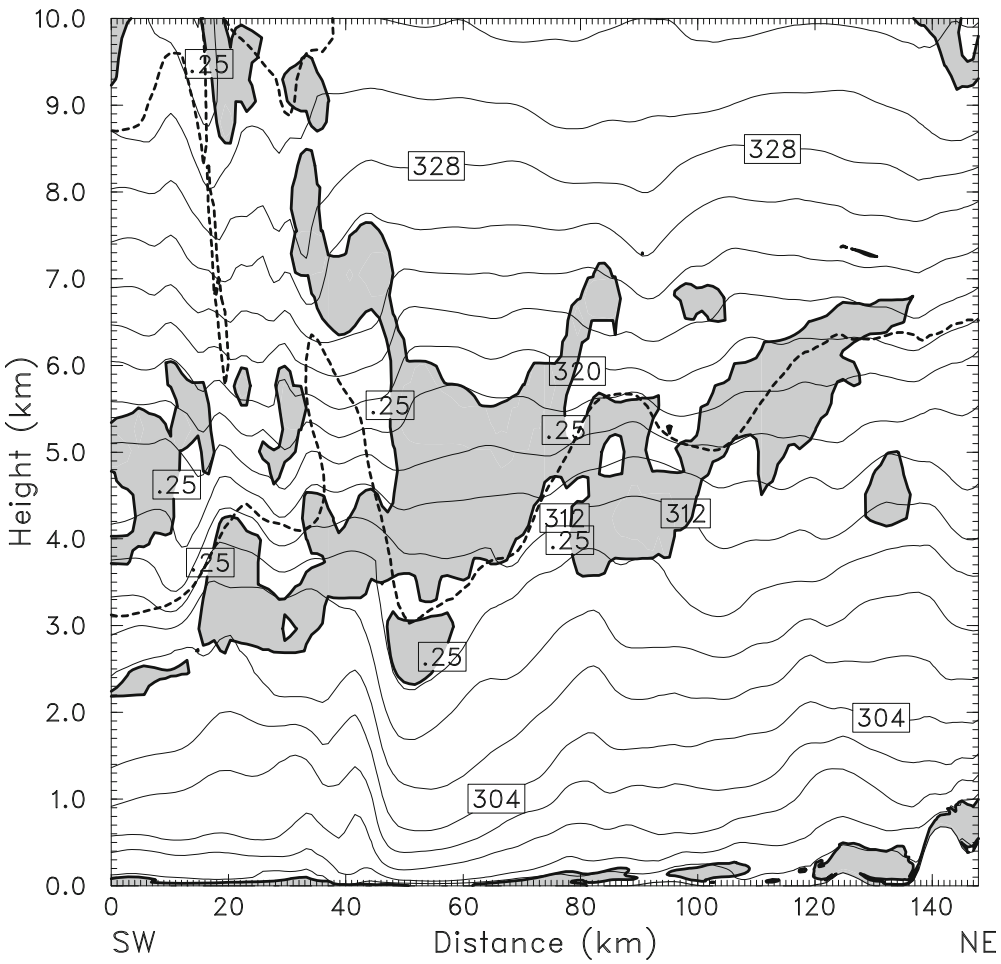

Figure 16
Vertical cross section of simulated potential temperature (solid black contours), Richardson number less than 0.25 (gray shaded) and wind speed contour of 30 m/s (dashed black contour) on 05:00 UTC 25 June 2014. Cross section is denoted in Fig. 9

propagated over the southern Adriatic. Therefore, persistent duct conditions were present during the Adriatic meteotsunami event.

Thus, both mechanisms, wave-CISK and wave duct, were at play to cause sustained and non-dissipative (or weakly dissipative) MSLP perturbations during this meteotsunami event. The convection that propagated from west to east and crossed Vela Luka bay was simulated, satisfying conditions which point to wave-CISK. Furthermore, environmental conditions for a wave duct were also satisfied, and an internal gravity wave packet, if created, could have been maintained through the wave duct mechanism. While there were no intensive internal gravity waves simulated at the time of Vela Luka meteotsunami, such a package was simulated a few hours later south of the Vela Luka area, and at a time of Rijeka Dubrovačka meteotsunami. It, therefore, seems that both convection and internal gravity waves embedded in a duct layer acted in concert during this event. The existence of both convection and wave duct conditions occurring during the meteotsunami events was documented earlier in the literature for the East China Sea (Tanaka 2010), while for the Adriatic, either the wave-CISK or wave duct was previously found to act as maintenance mechanisms of gravity waves (Belušić et al. 2007; Šepić et al. 2009). It is also likely that both convection and internal gravity waves originated or were at least modulated over the Apennines during the incoming (south)westerly flow. The investigation of the role of orography, its effect on organization of wave-like convection and internal gravity wave pattern is out of scope of this study, but certainly merits future work.

5. *Conclusions*

We investigated a major meteotsunami event that occurred in the Adriatic on 25 June 2014 using available sea-level and air pressure observations and by reproducing the event using the WRF model, with an aim to study atmospheric conditions conducive for the event. The meteotsunami sea-level oscillations were observed in several Adriatic harbors during the entire day, with maximal sea-level wave heights of $\sim$ 3 m observed in early morning in Vela Luka harbor, Korčula Island, Croatia. The special feature of this meteotsunami event is that it was a part of a series of individual meteotsunamis that occurred in the Mediterranean and Black Seas (Ciutadella harbor on Menorca Island, Spain, Mazzara del Valo harbor on Sicily, Italy and Odessa harbor in Ukraine) during period 23–27 June 2014 (Šepić et al. 2015).

Recorded observational evidence suggests sea-level oscillations in Vela Luka and other harbors were related to air pressure perturbations reaching amplitudes as large as 4 hPa. In the target area, these air pressure oscillations were collocated with clouds and precipitation of moderate intensity moving over the area. Satellite data suggest that wave-like cloud pattern of 20–40 km length scale was found over the Apennines but there was no clear evidence for existence of such structures over the Adriatic which could be also due to masking by other clouds and drying or moistening of the airflow. Nevertheless, those cloud structures were of appropriate scales to couple with the ocean surface and cause a meteotsunami. Furthermore, lightning data show that deep convection occurred early in the day and up to 1 h prior to the Vela Luka event, but that lightening activity and deep convection in an hour preceding the event in the Vela Luka area were much weaker and apparently limited to isolated convective cells.

We successfully simulated both rapid pressure oscillations and convection moving over the area in the simulation performed by the Weather Research and Forecasting model (WRF-ARW). Primary pressure oscillations were of similar amplitude as measured (around 4 hPa) at the very location of Vela Luka harbor. According to the model simulation, distance between crest and ridge of the pressure perturbations was approximately 25 km corresponding to length scales that are able to interact with the ocean surface through Proudman resonance. Simulated pressure perturbation structure was maintained for about an hour clearly demonstrating a potential to cause the meteotsunami.

Perturbations of vertical velocity associated with convective precipitation zone were slightly tilted with height in the mid- and upper troposphere. This suggests that a mechanism similar to wave-CISK was at play to maintain the precipitation zone and pressure perturbations over a required period of time. Besides

convection, model simulation points also to frequent occurrence of internal gravity waves. Such an internal gravity wave packet, not related to wave-CISK maintenance mechanism, was simulated to approach Rijeka Dubrovačka at the approximate time of the meteotsunami there. Further analysis suggests several conditions required for a wave duct were also satisfied: (1) low-level tropospheric air was statically stable, (2) this stable layer was topped by a sheared unstable layer with $R_i < 0.25$, (3) there was an embedded critical level for internal gravity waves in the unstable layer and (4) wave duct layer was 3.5 km deep—as required for a duct to occur. Therefore, both mechanisms, wave-CISK and wave duct, were at play to maintain mean sea-level pressure perturbations during this meteotsunami event. It, furthermore, appears that properties of both convection and internal gravity waves have been affected by a flow modulation over the Apennines.

Since all of these events occurred while a particular tsunamigenic synoptic situation was present over the entire Mediterranean, further analysis of meteotsunamis occurring in the other areas in days before and after the Adriatic event is of importance to synthesize conceptual models of meteotsunamis in the Mediterranean and the Black Seas. It is also important to assess the ability of numerical models to simulate atmospheric conditions during those events. While in several studies numerical models were short of simulating amplitude, location and structure of pressure perturbations in affected harbors, simulations performed in this event demonstrated reasonable model accuracy to represent the recorded pressure perturbations. This is, therefore, a step forward in demonstrating the ability of atmospheric mesoscale models for usage in coupled atmosphere–ocean numerical prediction systems for the purpose of early meteotsunami warning in the Mediterranean and the Black Seas.

Acknowledgements

We would like to thank all organisations that kindly provided us the data used in this study: European Centre for Middle-range Weather Forecast, Reading (http://www.ecmwf.int); European Organization for the Exploitation of Meteorological Satellites (http://www.eumetsat.int); Hydrographic Institute of the Republic of Croatia, Split; Institute of Oceanography and Fisheries, Split, Croatia; and Meteorological and Hydrological Service, Zagreb, Croatia. The work of KH and JS has been supported by the Croatian Science Foundation under the project MESSI (UKF Grant no. 25/15). MTP thanks the Croatian Science Foundation (HrZZ) project VITCLIC (PKP-2016-06-2975) which is funded by the Environmental Protection and Energy Efficiency Fund under the Government Program (Ministry of Environment and Energy and Ministry of Science and Education) for the Promotion of Research and Development Activities in the Field of Climate Change for the period 2015–2016.

References

Belušić, D., Grisogono, B., & Klaić, Z. B. (2007). Atmospheric origin of the devastating coupled air–sea event in the east Adriatic. *Journal of Geophysical Research, 112,* D17111. https://doi.org/10.1029/2006jd008204.

Belušić, D., & Strelec-Mahović, N. (2009). Detecting and following atmospheric disturbances with a potential to generate meteotsunamis in the Adriatic. *Physics and Chemistry of the Earth, 34,* 918–927.

Dudhia, J. (1989). Numerical study of convection observed during the winter monsoon experiment using a mesoscale two-dimensional model. *Journal of the Atmospheric Sciences, 46,* 3077–3107.

Dudhia, J. (1996). A multi-layer soil temperature model for MM5. The sixth PSU/NCAR mesoscale model Users' Workshop, pp. 22–24.

Horvath, K., Koracin, D., Vellore, R. K., Jiang, J., & Belu, R. (2012). Sub-kilometer dynamical downscaling of near-surface winds in complex terrain using WRF and MM5 mesoscale models. *Journal of Geophysical Research, 117,* D11111. https://doi.org/10.1029/2012jd017432.

Horvath, K., & Vilibić, I. (2014). Atmospheric mesoscale conditions during the Boothbay meteotsunami: A numerical sensitivity study using a high-resolution mesoscale model. *Natural Hazards, 74,* 55–74. https://doi.org/10.1007/s11069-014-1055-1.

Janjić, Z. I. (1994). The step-mountain eta coordinate model: Further developments of the convection, viscous sublayer, and turbulence closure schemes. *Monthly Weather Review, 122,* 927–945.

Kain, J. S. (2004). The Kain–Fritsch convective parameterization: An update. *Journal of Applied Meteorology, 43,* 170–181.

Kehler-Poljak, G., Telišman Prtenjak, M., Kvakić, M., Šariri, K., & Večenaj, Ž. (2017). Interaction of Sea breeze and deep convection over the Northeastern Adriatic coast: An analysis of sensitivity experiments using a high-resolution mesoscale model. *Pure and Applied Geophysics, 174,* 4197–4224. https://doi.org/10.1007/s00024-017-1607-x.

Lin, Y.-L. (2007). *Mesoscale dynamics* (p. 630). Cambridge: Cambridge University Press.

Lindzen, R. S. (1974). Wave-CISK in the tropics. *Journal of the Atmospheric Sciences, 31,* 156–179.

Lindzen, R. S., & Tung, K. K. (1976). Banded convective activity and ducted gravity waves. *Monthly Weather Review, 104,* 1602–1617.

Mlawer, E. J., Taubmanm, S. J., Brown, P. D., Iacono, M. J., & Clough, S. A. (1997). Radiative transfer for inhomogeneous atmospheres: RRTM, a validated correlated-k model for the longwave. *Journal of Geophysical Research, 102,* 16663–16682.

Monserrat, S., Vilibić, I., & Rabinovich, A. B. (2006). Meteotsunamis: Atmospherically induced destructive ocean waves in the tsunami frequency band. *Natural Hazards and Earth System Sciences, 6,* 1035–1051.

Morrison, H., Curry, J. A., & Khvorostyanov, V. I. (2005). A new double-moment microphysics parameterization for application in cloud and climate models, Part I: Description. *Journal of the Atmospheric Sciences, 62,* 1665–1677.

Orlić, M. (2015). The first attempt at cataloguing tsunami-like waves of meteorological origin in Croatian coastal waters. *Acta Adriatica, 56,* 83–96.

Orlić, M., Belušić, D., Janeković, I., & Pasarić, M. (2010). Fresh evidence relating the great Adriatic surge of 21 June 1978 to mesoscale atmospheric forcing. *Journal of Geophysical Research, 115,* C06011. https://doi.org/10.1029/2009JC005777.

Pawlowicz, R., Beardsley, B., Lentz, S., (2002). Classical tidal harmonic analysis including error estimates in MATLAB using T_TIDE. *Computers & Geosciences, 28,* 929–937.

Renault, L., Vizoso, G., Jansa, A., Wilkin, J., & Tintoré, J. (2011). Toward the predictability of meteotsunamis in the Balearic Sea using regional nested atmosphere and ocean models. *Geophysical Research Letters, 38,* L10601. https://doi.org/10.1029/2011GL047361.

Šepić, J., Međugorac, I., Janeković, I., Dunić, N., & Vilibić, I. (2016). Multi-meteotsunami event in the Adriatic Sea generated by atmospheric disturbances of 25–26 June 2014. *Pure and Applied Geophysics, 173*(12), 4117–4138. https://doi.org/10.1007/s00024-016-1249-4.

Šepić, J., Rabinovich, A. B., & Sytov, V. N. (2018a). Odessa tsunami of 27 June 2014: Observations and numerical modelling. *Pure and Applied Geophysics*. https://doi.org/10.1007/s00024-017-1729-1.

Šepić, J., Vilibić, I., & Belušić, D. (2009). The source of the 2007 Ist meteotsunami (Adriatic Sea). *Journal of Geophysical Research*. https://doi.org/10.1029/2008JC005092.

Šepić, J., Vilibić, I., Rabinovich, A. B., & Monserrat, S. (2015). Widespread tsunami-like waves of 23–27 June in the Mediterranean and Black Seas generated by high-altitude atmospheric forcing. *Scientific Reports, 5,* 11682. https://doi.org/10.1038/srep11682.

Šepić, J., Vilibić, I., Rabinovich, A. B., & Tinti, S. (2018b). Meteotsunami ("marrobbio") of 25–26 June on the southwestern coast of Sicily. *Pure and Applied Geophysics* **(submitted)**.

Skamarock, W. C., Klemp, J. B., Dudhia, J., Gill, D. O., Barker, D. M., Duda, M. G., et al. (2008). *A description of the advanced research WRF version 3, NCAR/TN-475?STR. Description of the WRF model*. Boulder: NCAR.

Tanaka, K. (2010). Atmospheric pressure-wave bands around a cold front resulted in a meteotsunami in the East China Sea in February 2009. *Natural Hazards and Earth System Sciences, 10,* 2599–2610.

Thomson, R. E., & Emery, W. J. (2014). *Data analysis methods in physical oceanography* (3rd ed., p. 716p). New York: Elsevier Science.

Vilibić, I. (2008). Numerical simulations of the Proudman resonance. *Continental Shelf Research, 28,* 574–581.

Vilibić, I., Domijan, N., Orlić, M., Leder, N., & Pasarić, M. (2004). Resonant coupling of a traveling air pressure disturbance with the east Adriatic coastal waters. *Journal of Geophysical Research, 109,* C10001. https://doi.org/10.1029/2004JC002279.

Vilibić, I., Horvath, K., StrelecMahovic, N., Monserrat, S., Marcos, M., Amores, A., et al. (2014). Atmospheric processes responsible for generation of the 2008 Boothbay meteotsunami. *Natural Hazards, 74,* 25–53. https://doi.org/10.1007/s11069-013-0811-y.

(Received December 5, 2017, revised February 28, 2018, accepted May 9, 2018)